

Realistic Bell tests with homodyne measurements

Enky Oudot,^{1,*} Gaël Massé,^{2,*} Xavier Valcarce,³ and Antonio Acín¹

¹*ICFO-Institut de Ciències Fotoniques, The Barcelona Institute of Science and Technology, Av. Carl Friedrich Gauss 3, 08860 Castelldefels (Barcelona), Spain*

²*LAAS-CNRS, Toulouse, France*

³*Université Paris-Saclay, CEA, CNRS, Institut de physique théorique, 91191, Gif-sur-Yvette, France*

We analyze Bell inequalities violations in photonic experiments for which the measurement apparatuses are restricted to homodyne measurements. Through numerical optimization of the Clauser-Horne-Shimony-Holt inequality over homodyne measurements and binning choices, we demonstrate large violations for states with a bounded number of photons. When considering states defined within qubit local subspaces of two Fock states, such as NOON states, a violation is observed solely within the qubit Fock space spanned by zero and two photons. For more generic states, large violations are obtained. Significant violations are observed even for states containing three photons locally and under realistic values of noise and losses. We propose concrete implementations to achieve such violations, opening new avenues for Bell experiments with homodyne detectors.

I. INTRODUCTION

Bell inequalities serve as a powerful tool to demonstrate the incompatibility of quantum predictions with classical models in which measurements are pre-determined [1, 2]. Initially explored for its foundational implications, Bell nonlocality has now emerged as the core resource for quantum information processing in a *device-independent* (DI) manner, *i.e.* without making assumptions about the underlying quantum model. Notably, nonlocality has been leveraged to certify quantum resources, thanks to self-testing [3, 4], and to provide device-independent security proofs for quantum key distribution [5–11].

DI protocols require a violation of a Bell inequality, with the Clauser-Horne-Shimony-Holt (CHSH) inequality being the most iconic [12]. Bell tests have been successfully conducted [13–18], and some DI protocols have seen their first realizations [19–22]. However, so far these tests involve measurements devices relying on superconducting nanowire single-photon detectors, which require cryogenic temperatures to operate efficiently. This stands in contrast with the practical and commercial expectations for the implementation of DI protocols, where on-chip integration is highly desirable.

We here seek to find set-ups that can achieve large CHSH violations with standard photonic devices. Thanks to their high efficiency, homodyne detectors are considered promising to close the detection loophole. Moreover, they fulfill two important criteria for practical Bell tests: being adapted to telecom wavelength and being able to include integrable detectors. Wenger *et al.* showed that one can find arbitrarily high violations of CHSH, based on continuous variables [23]. This result was also generalised to the multipartite case in [24]. Unfortunately, the states proposed to attain the maximal CHSH violation are not fitted for experimental imple-

mentations. On the other hand, the authors of [25, 26] proposed a setup, using photon subtraction on a two-mode squeezed state, that leads to a CHSH value of $S \approx 2.048$. While the required state is feasible in present experiments, the reported violation is fairly small and thus of limited use for DI applications. The situation is therefore as follows: too small violations have been obtained for realistic setups, while large, and even optimal violations are possible for states completely out of reach. This work reduces the gap between experimental feasibility and high violation of Bell inequalities.

In this manuscript, we derive Bell violations for the CHSH inequality using homodyne measurements. Notably, we found violations that are significantly larger than those found in previous works for realistic and robust experiments. After a brief reminder on Bell scenarios and on homodyne apparatuses in Sec. II, we explore violations of the CHSH inequality in local qubit Fock spaces in Sec. III. We then consider local qudit Fock spaces of growing dimensions. For each case, we give the CHSH score optimised over measurement parameters in Sec. IV, and an analysis of the robustness considering a realistic noise model in Sec. V. Finally, in Sec. VI we propose experimental set-ups that implement some of the violations derived in the precedent sections.

II. PRELIMINARIES

A. Bell scenarios

We consider a scenario in which two distant users, Alice and Bob receive correlated particles from a source. Each one can select locally a measurement indexed by x, y over a choice of m different ones. Each measurement can yield Δ possible outcomes [2] noted a for Alice and b for Bob. By repeating this protocol and sharing the results, it is possible to compute the conditional probabilities of obtaining outcomes knowing the local choices of measurements, written $P_{AB}(a, b|x, y)$. Probabilities com-

* These two authors contributed equally

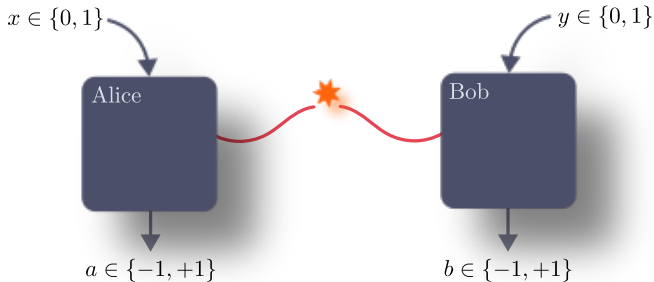


FIG. 1. Schematic representation of a bipartite Bell test. In each round, Alice and Bob independently chose a setting x and y and perform the corresponding measurement on the shared state. Then, they record their respective outcome a and b . After many rounds, they compute the statistics $P_{AB}(ab|xy)$ from their choice of settings and outcomes.

patible with a local hidden variable (LHV) model can be expressed as

$$P_{AB}^{\text{loc}}(a, b|x, y) = \int_{\lambda} P(\lambda) P_A(a|\lambda, x) P_B(b|\lambda, y) d\lambda. \quad (1)$$

Such distributions are called *local*. A Bell inequality is an upper-bound on a linear combination of the probabilities $P_{AB}(a, b|x, y)$, given by the maximum value achievable with probability distributions of the form Eq. (1).

B. The CHSH inequality

In this article, we consider bipartite Bell inequalities, with a focus on the simplest non trivial scenario. Each party can chose between two measurements, while the outcomes they obtain can take two values, either -1 or 1 , as depicted in Fig. 1. In this case, there exists only one Bell inequality, the so-called Clauser-Horne-Shimony-Holt (CHSH) inequality [12] which reads

$$\langle \mathcal{B}_{\text{CHSH}} \rangle = \langle A_0 B_0 \rangle + \langle A_0 B_1 \rangle + \langle A_1 B_0 \rangle - \langle A_1 B_1 \rangle \leq 2. \quad (2)$$

with $\langle A_x B_y \rangle = \sum_{a,b} p(a = b|x, y) - p(a \neq b|x, y)$, and where $A_i (B_j)$ stands for measurements by Alice (respectively Bob). The local bound of the CHSH inequality is 2 whereas the maximum value predicted by quantum theory reaches $2\sqrt{2}$ [27]. Note that in section IV and V, we explore violations of other Bell inequalities, when considering that Alice and Bob have access to more than two measurement settings.

C. Bell test with homodyne measurement

An homodyne measurement quantifies quadratures of the electromagnetic field. It corresponds to the measure of the operator

$$\hat{X}_{\theta} = \frac{\hat{a}e^{-i\theta} + \hat{a}^{\dagger}e^{i\theta}}{2}, \quad (3)$$

where \hat{a} and \hat{a}^{\dagger} are the ladder operators, and with $\theta \in [0, 2\pi]$. Note that the operator \hat{X}_{θ} has a spectrum in \mathbb{R} . In order to step in the framework of a Bell test, a transformation from \mathbb{R} into $\{-1, 1\}$ is necessary. This is called *binning*. The positive operator-valued measure (POVM) elements corresponding to binned measurements read

$$\{\prod_{+1}^{\theta, I}, \prod_{-1}^{\theta, I}\} = \left\{ \int_I dX_{\theta} |X_{\theta}\rangle \langle X_{\theta}|, \int_{\bar{I}} dX_{\theta} |X_{\theta}\rangle \langle X_{\theta}| \right\} \quad (4)$$

where $|X_{\theta}\rangle$ is an eigenstate of the generalized quadrature \hat{X}_{θ} , I is a set of \mathbb{R} and \bar{I} is its complementary. The observable corresponding to such POVM elements is

$$\sigma^{\theta, I} = \prod_{+1}^{\theta, I} - \prod_{-1}^{\theta, I}. \quad (5)$$

One can thus write the CHSH operator as

$$\mathcal{B}_{\text{CHSH}} = \sigma_{A1}^{\theta_{A1}, I_{A1}} \sigma_{B1}^{\theta_{B1}, I_{B1}} + \sigma_{A1}^{\theta_{A1}, I_{A1}} \sigma_{B2}^{\theta_{B2}, I_{B2}} + \sigma_{A2}^{\theta_{A2}, I_{A2}} \sigma_{B1}^{\theta_{B1}, I_{B1}} - \sigma_{A2}^{\theta_{A2}, I_{A2}} \sigma_{B2}^{\theta_{B2}, I_{B2}} \quad (6)$$

where $\vec{\theta} = \{\theta_{A0}, \theta_{A1}, \theta_{B0}, \theta_{B1}\}$ is the vector of the phase space direction of each measurement.

III. VIOLATION OF THE CHSH INEQUALITY WITH HOMODYNE MEASUREMENT IN LOCAL QUBIT FOCK SPACES

In this section, we focus on the Hilbert qubit space \mathcal{H}^2 spanned by the Fock states $\{|l\rangle, |m\rangle\}$. These basis represents states containing exactly l and m photons respectively. We start by extracting analytical lower bounds on the CHSH violation from the expression of the POVM elements. We then implement a numerical optimization to systematically explore higher possible CHSH violation.

A. CHSH Score from the POVM Elements

Any 2-outcome qubit POVM can be written

$$\begin{aligned} E_1 &= \mu |\vec{n}\rangle \langle \vec{n}| + (1 - \mu)r_1 \mathbb{1}, \\ E_2 &= \mu |-\vec{n}\rangle \langle -\vec{n}| + (1 - \mu)r_2 \mathbb{1}, \end{aligned} \quad (7)$$

where $\mu \in \{0, 1\}$ and $r_1 = 1 - r_2 \in \{0, 1\}$ quantifies the projective and the random part of the measurement respectively, and $|\pm\vec{n}\rangle$ are two orthogonal states in \mathcal{H}^2 (see Appendix A). μ relates to the ability of the POVM to distinguish between two orthogonal states, which is a necessary condition to violate the CHSH inequality. Therefore, maximizing μ in POVM's expressions might lead to higher CHSH score.

The projective part μ in direction $|\pm\vec{n}\rangle$ can be expressed following

$$\mu = \frac{1}{2} (\langle +\vec{n}| E_1 |+\vec{n}\rangle + \langle -\vec{n}| E_2 |-\vec{n}\rangle - 1). \quad (8)$$

Using the POVM expression for binned homodyne measurement defined in Eq. (4), we have

$$\mu_h = \frac{1}{2} \left(\int_I dX_\theta p(\theta, |+\vec{n}\rangle) + \int_{\bar{I}} p(\theta, |-\vec{n}\rangle) dX_\theta - 1 \right) \quad (9)$$

where $p(\theta, |\pm\vec{n}\rangle) = |\langle X_\theta | \pm\vec{n} \rangle|^2$. From this expression, we deduce that the maximum value of μ_h is reached when the set I is composed of the intervals of \mathbb{R} for which the inequality $p(\theta, |+\vec{n}\rangle) > p(\theta, |-\vec{n}\rangle)$ is satisfied. For this binning choice, μ_h can be computed from the trace distance between the two probability distributions $p(\theta, |\pm\vec{n}\rangle)$ and $p(\theta, |\pm\vec{n}\rangle)$. The maximum value of μ_h over the phase space direction θ and states $|\vec{n}\rangle$ is therefore given by

$$\max_{\theta, |\vec{n}\rangle} \frac{1}{2} \int \|p(\theta, |+\vec{n}\rangle) - p(\theta, |-\vec{n}\rangle)\| dX_\theta. \quad (10)$$

The maximum value of Eq. (10) is achieved for $\theta = 0$ and real orthogonal states $|\pm n\rangle$

$$|+\vec{n}\rangle = \cos(a) |l\rangle + \sin(a) |m\rangle \quad (11)$$

$$|-\vec{n}\rangle = \cos(a) |l\rangle - \sin(a) |m\rangle \quad (12)$$

where $a \in [0, 2\pi]$ (see Appendix A).

Moreover, we show in Appendix A that in the case where Alice and Bob use the same binning, for all μ_h such that $|\cos(2a)| \leq \frac{1}{2}$, a CHSH score of

$$S = \mu_h^2 2\sqrt{2} \quad (13)$$

can always be achieved. Consequently, the task of optimizing the trace distance between two phase space probability distributions of two orthogonal states boils down to optimizing a function of only one real parameter a . We optimize the value of this CHSH score for qubit Fock states $\{|l\rangle, |m\rangle\}$ going from $|0\rangle$ to $|7\rangle$. Surprisingly, the only space where we found a violation is the space spanned by $\{|0\rangle, |2\rangle\}$. In this case, the maximization of the CHSH score can be performed analytically and leads to $S \approx 2.1477$, obtained for the state

$$|\psi\rangle = \alpha |00\rangle + \beta |02\rangle + \beta |20\rangle + \alpha |22\rangle, \quad (14)$$

with $\alpha \approx -0.6504 - 0.0466i$, $\beta \approx 0.0124 - 0.2514i$, and for a binning defined by $I = [-0.8886, 0.8886]$.

B. Numerical optimization

We consider the eigenstate $|\psi\rangle$ and the eigenvalue λ of the CHSH operator

$$\mathcal{B}_{\text{CHSH}} |\psi\rangle = \lambda |\psi\rangle. \quad (15)$$

Since all quantum states can be decomposed in a basis of the eigenvectors of $\mathcal{B}_{\text{CHSH}}$, optimizing the CHSH score over all quantum states can be written

$$\max_{\psi} \langle \psi | \mathcal{B}_{\text{CHSH}} | \psi \rangle = \lambda_{\text{max}}, \quad (16)$$

where λ_{max} is the highest eigenvalue of $\mathcal{B}_{\text{CHSH}}$. Using Eq. (6), we deduce that λ_{max} depends on the choices of the binning I and the phase space directions of measurements θ of Alice and Bob. For measurements $\{A_x, B_x\}$, we define the binning strategy for a set I_x reading

$$I_x = [a_0^x, a_1^x] \cup [a_2^x, a_3^x] \cup \dots \cup [a_{q-1}^x, a_q^x] \quad (17)$$

with $\{a_0^x, a_1^x, \dots, a_q^x\} = \vec{a}_q^x \in \mathbb{R}^{q+1}$. We aim to find

$$\max_{\vec{\theta}, \vec{a}_q^0, \vec{a}_q^1} \text{Eig}(\mathcal{B}_{\text{CHSH}}). \quad (18)$$

As the choice of q directly impacts the optimization result, we performed optimizations over a growing number of binning elements until a similar score S is reached for q and $q+1$.

We run optimization Eq. (18) on qubit spaces spanned by Fock states $\{|l\rangle, |m\rangle\}$ up to $l, m = 20$. In all cases except $\{|0\rangle, |2\rangle\}$, the maximum score we obtain saturates the local bound. It is because a binning strategy such that the probability of getting the outcome $+1$ is 1 leads to a CHSH score of 2 in all cases. This is consistent with the results derived in the previous section. In the $\{|0\rangle, |2\rangle\}$ case, compared to the analytical method, we slightly improved the score to $S \approx 2.1493$. This improvement originates from a more refined binning choice, as different binning are allowed for measurements A_0, B_0 and A_1, B_1 . These binning are given by $I_0 = [-0.8886, 0.8854]$ and $I_1 = [-0.8689, 0.8679]$ respectively.

These two approaches strongly indicate that for qubit Fock spaces with up to 20 photons locally, no CHSH violation using homodyne measurement can be found except for the qubit Fock space $\{|0\rangle, |2\rangle\}$.

IV. CHSH SCORE FROM HOMODYNE MEASUREMENTS IN QUDIT FOCK SPACE

In this section, we extend the numerical optimization defined in Sec. III B to qudit Fock spaces. We first compute optimized CHSH scores for states of local dimension up to 10 in Sec. IV A before restricting to energy conserving states in Sec. IV B.

A. CHSH scores with homodyne measurements in local dimensions 3 to 10

For a local dimension d , we consider the Fock space spanned by the basis $\{|0\rangle, \dots, |d-1\rangle\}$. The state shared

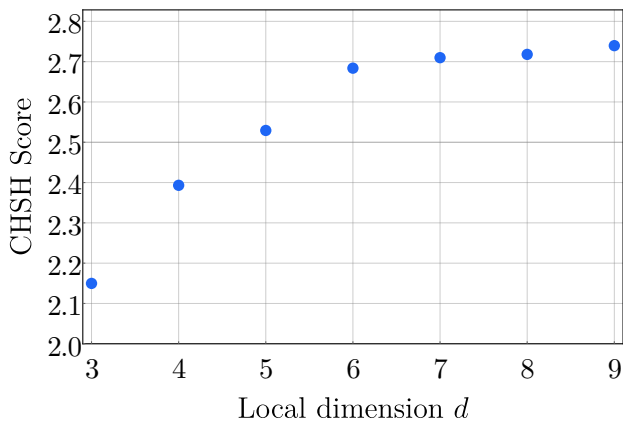


FIG. 2. Maximum possible quantum values for the CHSH inequality as a function of the local dimension of the observables. These results are certified with a numerical observation. Note that in dimension 3 we retrieve the score ≈ 2.14 derived in Sec. III.

between Alice and Bob is, therefore, a two-qudit state that lives in $\mathcal{H}^{d \times d}$. We run optimizations up to a maximum dimension of $d = 9$ as it corresponds to an upper bound of what can be possibly crafted with today's state of the art squeezing devices [28].

The maximum CHSH scores we obtained for various local dimensions are given in Fig 2. We observe that the larger the space dimension we consider, the larger the score. In local dimension $d = 3$, we retrieve the result of the $\{|0\rangle, |2\rangle\}$ space, leading to a score of $S \approx 2.14$. In dimension $d = 9$, we found a state yielding a score of $S \approx 2.7397$, close to the quantum bound.

B. Quantum bounds for energy-conserving states

We consider the specific case of optimizing the CHSH score in the case of energy-conserving states, due to their relevance for experimental implementation. In the case of a maximum number of 2 photons, it means that the observables are 3×3 matrices in the basis $\{|02\rangle, |11\rangle, |20\rangle\}$; with a maximum number of 3 photons, the observables are 4×4 matrices in the basis $\{|03\rangle, |12\rangle, |21\rangle, |30\rangle\}$, and so on and so forth. We verified that none of these constructions can yield a violation up to dimension 5.

V. ROBUSTNESS WITH RESPECT TO NOISE

Up until now we have considered ideal situations. However, in real-life, several factors generate so-called noise in experiments. For photonic experiment the leading source of noise is amplitude-damping. In this section, we study the robustness of the CHSH test with respect to losses.

We model photon losses by entangling an ideal incoming state with an ancillary fluctuating quantum field that

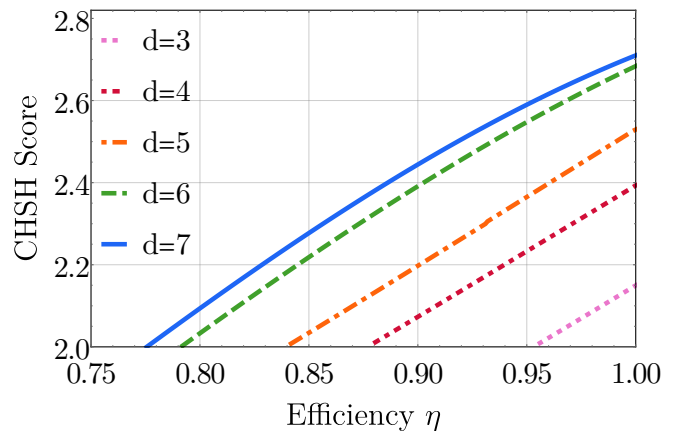


FIG. 3. Result of the optimization Eq. (20) yielding a CHSH score with respect to the overall efficiency of the protocol η . We plot the curves of the different ordered local Fock spaces $\{|0\rangle, \dots, |d\rangle\}$.

we set to the vacuum state $|0\rangle$. After recombination on a beam-splitter, two outputs are produced corresponding to the transmitted part of the beam-splitter and to the reflected one. In order to obtain the noisy operator, we trace-out the part corresponding to the reflection. Hence, stemming from the ideal observable Eq. (5), we get the noisy observable

$$\sigma_{A,\eta}^{\theta,I} = \langle 0 | \hat{U} \sigma_A^{\theta,I} \hat{U}^\dagger | 0 \rangle \quad (19)$$

where \hat{U} is the beam-splitter observable defined by $\hat{U} = e^{i\gamma(\hat{a}^\dagger \hat{b} - \hat{a} \hat{b}^\dagger)}$, \hat{a}, \hat{b} are the annihilation operators respectively on the first and second mode, and the reflectivity of the beam splitter is $\eta = \cos(\gamma)^2$ (see Appendix B for the derivation). In this way, we construct a new Bell operator $\mathcal{B}_{\text{CHSH}}^\eta$ by replacing $\sigma_i^{\theta,I}$ with $\sigma_{i,\eta}^{\theta,I}$ in Eq. (6).

We thus perform the optimization

$$\max_{\vec{\theta}, \vec{a}_i^n} \text{Eig}(\mathcal{B}_{\text{CHSH}}^\eta). \quad (20)$$

This allow us to obtain a threshold efficiency η_c that depends on the incremental dimension of the space tested. We display the result of this optimization in Fig 3. We see that by going to higher dimension one can increase the losses robustness of the CHSH violation. In the space spanned by $\{|0\rangle, \dots, |6\rangle\}$ we obtain a robustness of $\eta_c \approx 0.77$ for the losses.

Additionally, we explore the robustness to losses for scenarios where Alice and Bob have up to 4 local measurement settings. All the 175 Bell inequalities of these scenarios can be found in [29]. We compute the optimisation Eq. (20) for all of them. Interestingly, for all tested local dimensions, no inequalities yield a better threshold efficiency η_c than the CHSH inequality.

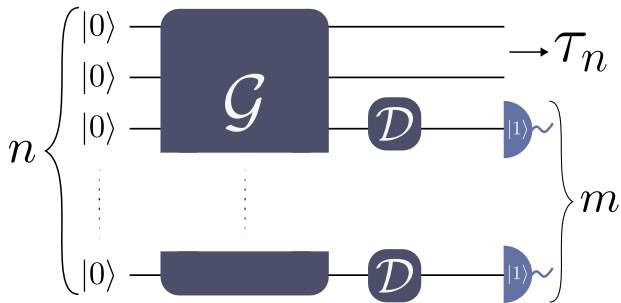


FIG. 4. n -mode bosonic parameterized circuits. The modes are initialized to the vacuum $|0\rangle$. A Gaussian process \mathcal{G} is applied on all modes. $m = n - 2$ displacement operations \mathcal{D} are performed on the last modes, before heralding operations on single photon count. The state τ_n is then send to Alice and Bob.

VI. REALISTIC IMPLEMENTATION

To emphasize our results, we study the experimental implementation of quantum states ρ_d yielding the highest CHSH score, for some of the maximum local dimensions constraints d . We consider implementations based on Gaussian processes and heralding operations using photon-number resolving (PNR) detectors. More specifically, we focus on n bosonic modes circuits in which a n -mode Gaussian unitary transformation with zero-displacement, \mathcal{G} , is applied, followed by real displacements operations on every but the first two modes, see Appendix C. The $m = 2 - n$ last modes are then heralded on single photon count, while the first two modes output a final state τ_n send to Alice and Bob. Fig. 4 represents the photonic circuits under consideration.

Note that the Gaussian process \mathcal{G} can be realistically implemented using an array of single mode squeezers followed by passive non linear optics, combining beam-splitters and phase shifters [30–32]. Moreover, recent results display successful implementations of heralding systems using PNR detectors [33, 34].

We optimize the fidelity $F(\rho_d, \tau_n)$ over the Gaussian process and the displacement operations. This is achieved using the Riemannian optimization on the symplectic group described in [35] and implemented in the MRMUSTARD library [36]. Due to convergence instability with a higher number of modes n , we perform this optimization multiple times to avoid local minimum.

We focus on target states ρ_d with maximum local dimensions $d = \{3, 4\}$. For each target state, we optimize circuits composed of 3 to 7 modes. In Appendix C, we provide the optimized fidelities and the corresponding squeezing and displacement parameters. Importantly, these parameters are within the realm of experimental feasibility.

For $d = 3$, the target state ρ_3 which achieves a CHSH score of $S \approx 2.14$ can be exactly prepared using a circuit with $n \geq 6$ modes. For $d = 4$, with a maximum number

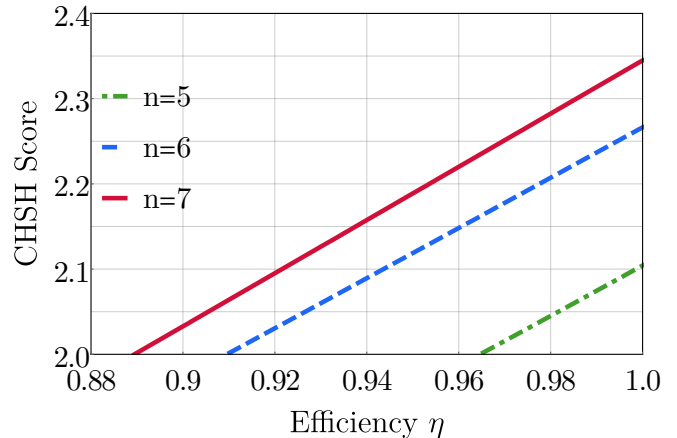


FIG. 5. CHSH Score optimized over measurement and binning choices for state τ_n obtained by maximizing $F(\rho_{d=4}, \tau_n)$. Results are given for circuits with 5,6 and 7 bosonic modes.

of $n = 7$ mode, we are able to match the fidelity up to $F(\rho_4, \tau_7) \approx 0.983$. After optimizing the measurement directions and binning choices, the state ρ_7 achieves a high CHSH score of $S \approx 2.34$.

Finally, we study the robustness to losses for some of these state preparations. In the $d = 3$ case, considering the $n \geq 6$ -modes circuits, we recovered the results obtained using the optimization of Eq. (20). In Fig. 5, we show the evolution of the CHSH score optimized over binning and measurement choices for the state prepared with circuit targeting the ρ_4 state.

CONCLUSION

In this work we consider the task of violating Bell inequalities using homodyne measurements. In local qubit Fock spaces, we develop a method that suggests the CHSH inequality is violated only in the space spanned by 0 and 2 photons. Then we consider local qudit Fock spaces of increasing dimensions and optimize the CHSH score in each case. We found states that yield the largest violations observed in the literature for a fixed dimension. We focus on the experimental feasibility, first by deriving thresholds of efficiency required to enable Bell inequalities violations, then by proposing realistic set-ups which can produce such violations. We believe that this represents a significant step towards a Bell experiment with homodyne measurements. Future works include considering POVMs of more than 2 outcomes, extending our results to the cases of heterodyne measurements and exploring the feasibility of device-independent protocol, including DIQKD, with homodyne measurements.

ACKNOWLEDGMENTS

This work was supported by the FastQI grant funded by the Institut Quantique Occitan. E.O acknowledges support from the Government of Spain (FIS2020-TRANQI and Severo Ochoa CEX2019-000910-S), Fundació Cellex, Fundació Mir-Puig, Generalitat de Catalunya (CERCA, AGAUR SGR 1381) and from the ERC AdGCERQUT. X.V. acknowledges funding by the

European Union’s Horizon Europe research and innovation program under the project “Quantum Security Networks Partnership” (QSNP, Grant Agreement No. 101114043) and by a French national quantum initiative managed by Agence Nationale de la Recherche in the framework of France 2030 with the reference ANR-22-PETQ-0009.

-
- [1] John S Bell, “On the Einstein-Podolsky-Rosen paradox,” *Physics* **1**, 195–200 (1964).
- [2] Nicolas Brunner, Daniel Cavalcanti, Stefano Pironio, Valerio Scarani, and Stephanie Wehner, “Bell nonlocality,” *Rev. Mod. Phys.* **86**, 419–478 (2014).
- [3] Dominic Mayers and Andrew Yao, “Self testing quantum apparatus,” *Quantum Info. Comput.* **4**, 273–286 (2004).
- [4] Ivan Šupić and Joseph Bowles, “Self-testing of quantum systems: a review,” *Quantum* **4**, 337 (2020).
- [5] Antonio Acín, Nicolas Brunner, Nicolas Gisin, Serge Massar, Stefano Pironio, and Valerio Scarani, “Device-independent security of quantum cryptography against collective attacks,” *Physical Review Letters* **98** (2007), 10.1103/physrevlett.98.230501.
- [6] Stefano Pironio, Antonio Acín, Nicolas Brunner, Nicolas Gisin, Serge Massar, and Valerio Scarani, “Device-independent quantum key distribution secure against collective attacks,” *New Journal of Physics* **11**, 045021 (2009).
- [7] Umesh Vazirani and Thomas Vidick, “Fully device-independent quantum key distribution,” *Physical Review Letters* **113** (2014), 10.1103/physrevlett.113.140501.
- [8] Pavel Sekatski, Jean-Daniel Bancal, Xavier Valcarce, Ernest Y.-Z. Tan, Renato Renner, and Nicolas Sangouard, “Device-independent quantum key distribution from generalized CHSH inequalities,” *Quantum* **5**, 444 (2021).
- [9] Víctor Zapatero and Marcos Curty, “Long-distance device-independent quantum key distribution,” *Scientific Reports* **9**, 17749 (2019).
- [10] René Schwonnek, Koon Tong Goh, Ignatius W. Primaatmaja, Ernest Y.-Z. Tan, Ramona Wolf, Valerio Scarani, and Charles C.-W. Lim, “Device-independent quantum key distribution with random key basis,” *Nature Communications* **12** (2021), 10.1038/s41467-021-23147-3.
- [11] Víctor Zapatero, Tim van Leent, Rotem Arnon-Friedman, Wen-Zhao Liu, Qiang Zhang, Harald Weinfurter, and Marcos Curty, “Advances in device-independent quantum key distribution,” *npj Quantum Information* **9**, 10 (2023).
- [12] John F. Clauser, Michael A. Horne, Abner Shimony, and Richard A. Holt, “Proposed experiment to test local hidden-variable theories,” *Phys. Rev. Lett.* **23**, 880–884 (1969).
- [13] Marissa Giustina, Marijn AM Versteegh, Sören Wengerowsky, Johannes Handsteiner, Armin Hochrainer, Kevin Phelan, Fabian Steinlechner, Johannes Kofler, Jan-Åke Larsson, Carlos Abellán, *et al.*, “Significant loophole-free test of bell’s theorem with entangled photons,” *Physical review letters* **115**, 250401 (2015).
- [14] B. Hensen, H. Bernien, A. E. Dréau, A. Reiserer, N. Kalb, M. S. Blok, J. Ruitenberg, R. F. L. Vermeulen, R. N. Schouten, C. Abellán, W. Amaya, V. Pruneri, M. W. Mitchell, M. Markham, D. J. Twitchen, D. Elkouss, S. Wehner, T. H. Taminiau, and R. Hanson, “Loophole-free bell inequality violation using electron spins separated by 1.3 kilometres,” *Nature* **526**, 682–686 (2015).
- [15] Lynden K Shalm, Evan Meyer-Scott, Bradley G Christensen, Peter Bierhorst, Michael A Wayne, Martin J Stevens, Thomas Gerrits, Scott Glancy, Deny R Hamel, Michael S Allman, *et al.*, “Strong loophole-free test of local realism,” *Physical review letters* **115**, 250402 (2015).
- [16] Wenjamin Rosenfeld, Daniel Burchardt, Robert Garthoff, Kai Redeker, Norbert Ortengel, Markus Rau, and Harald Weinfurter, “Event-ready bell test using entangled atoms simultaneously closing detection and locality loopholes,” *Physical Review Letters* **119** (2017), 10.1103/physrevlett.119.010402.
- [17] Ming-Han Li, Cheng Wu, Yanbao Zhang, Wen-Zhao Liu, Bing Bai, Yang Liu, Weijun Zhang, Qi Zhao, Hao Li, Zhen Wang, Lixing You, W. J. Munro, Juan Yin, Jun Zhang, Cheng-Zhi Peng, Xiongfang Ma, Qiang Zhang, Jingyun Fan, and Jian-Wei Pan, “Test of local realism into the past without detection and locality loopholes,” *Physical Review Letters* **121** (2018), 10.1103/physrevlett.121.080404.
- [18] Simon Storz, Josua Schär, Anatoly Kulikov, Paul Magnard, Philipp Kurpiers, Janis Lütolf, Theo Walter, Adrian Copetudo, Kevin Reuer, Abdulkadir Akin, Jean-Claude Besse, Mihai Gabureac, Graham J. Norris, Andrés Rosario, Ferran Martin, José Martínez, Waldimar Amaya, Morgan W. Mitchell, Carlos Abellán, Jean-Daniel Bancal, Nicolas Sangouard, Baptiste Royer, Alexandre Blais, and Andreas Wallraff, “Loophole-free bell inequality violation with superconducting circuits,” *Nature* **617**, 265–270 (2023).
- [19] Yang Liu, Qi Zhao, Ming-Han Li, Jian-Yu Guan, Yanbao Zhang, Bing Bai, Weijun Zhang, Wen-Zhao Liu, Cheng Wu, Xiao Yuan, Hao Li, W. J. Munro, Zhen Wang, Lixing You, Jun Zhang, Xiongfang Ma, Jingyun Fan, Qiang Zhang, and Jian-Wei Pan, “Device-independent quantum random-number generation,” *Nature* **562**, 548–551 (2018).
- [20] Wen-Zhao Liu, Yu-Zhe Zhang, Yi-Zheng Zhen, Ming-Han Li, Yang Liu, Jingyun Fan, Feihu Xu, Qiang Zhang, and Jian-Wei Pan, “Toward a photonic demonstration of device-independent quantum key distribu-

- tion,” *Physical Review Letters* **129** (2022), 10.1103/physrevlett.129.050502.
- [21] Wei Zhang, Tim van Leent, Kai Redeker, Robert Garthoff, René Schwonnek, Florian Fertig, Sebastian Eppelt, Wenjamin Rosenfeld, Valerio Scarani, Charles C.-W. Lim, and Harald Weinfurter, “A device-independent quantum key distribution system for distant users,” *Nature* **607**, 687–691 (2022).
- [22] D. P. Nadlinger, P. Drmota, B. C. Nichol, G. Araneda, D. Main, R. Srinivas, D. M. Lucas, C. J. Ballance, K. Ivanov, E. Y.-Z. Tan, P. Sekatski, R. L. Urbanke, R. Renner, N. Sangouard, and J.-D. Bancal, “Experimental quantum key distribution certified by bell’s theorem,” *Nature* **607**, 682–686 (2022).
- [23] Jérôme Wenger, Mohammad Hafezi, Frédéric Grosshans, Rosa Tualle-Brouri, and Philippe Grangier, “Maximal violation of bell inequalities using continuous-variable measurements,” *Physical Review A* **67** (2003), 10.1103/physreva.67.012105.
- [24] Antonio Acín, Nicolas J. Cerf, Alessandro Ferraro, and Julien Niset, “Tests of multimode quantum nonlocality with homodyne measurements,” *Phys. Rev. A* **79**, 012112 (2009).
- [25] R. García-Patrón, J. Fiurášek, N. J. Cerf, J. Wenger, R. Tualle-Brouri, and Ph. Grangier, “Proposal for a loophole-free bell test using homodyne detection,” *Physical Review Letters* **93** (2004), 10.1103/physrevlett.93.130409.
- [26] Raúl García-Patrón, Jaromír Fiurášek, and Nicolas J. Cerf, “Loophole-free test of quantum nonlocality using high-efficiency homodyne detectors,” *Physical Review A* **71** (2005), 10.1103/physreva.71.022105.
- [27] B. S. Tsirel’son, “Quantum analogues of the bell inequalities. the case of two spatially separated domains,” *Journal of Soviet Mathematics* **36**, 557–570 (1987).
- [28] Henning Vahlbruch, Moritz Mehmet, Karsten Danzmann, and Roman Schnabel, “Detection of 15 db squeezed states of light and their application for the absolute calibration of photoelectric quantum efficiency,” *Physical Review Letters* **117** (2016), 10.1103/physrevlett.117.110801.
- [29] Enky Oudot, Jean-Daniel Bancal, Pavel Sekatski, and Nicolas Sangouard, “Bipartite nonlocality with a many-body system,” *New Journal of Physics* **21**, 103043 (2019).
- [30] Claude Bloch and Albert Messiah, “The canonical form of an antisymmetric tensor and its application to the theory of superconductivity,” *Nuclear Physics* **39**, 95–106 (1962).
- [31] Samuel L. Braunstein, “Squeezing as an irreducible resource,” *Phys. Rev. A* **71**, 055801 (2005).
- [32] Gianfranco Cariolaro and Gianfranco Pierobon, “Bloch-messiah reduction of gaussian unitaries by takagi factorization,” *Phys. Rev. A* **94**, 062109 (2016).
- [33] Samantha I. Davis, Andrew Mueller, Raju Valivarthi, Nikolai Lauk, Lautaro Narvaez, Boris Korzh, Andrew D. Beyer, Olmo Cerri, Marco Colangelo, Karl K. Berggren, Matthew D. Shaw, Si Xie, Neil Sinclair, and Maria Spiropulu, “Improved heralded single-photon source with a photon-number-resolving superconducting nanowire detector,” *Phys. Rev. Appl.* **18**, 064007 (2022).
- [34] Lorenzo Stasi, Patrik Caspar, Tiff Brydges, Hugo Zbinden, Félix Bussi eres, and Rob Thew, “High-efficiency photon-number-resolving detector for improving heralded single-photon sources,” *Quantum Science and Technology* **8**, 045006 (2023).
- [35] Yuan Yao, Filippo Miatto, and Nicol as Quesada, “On the design of photonic quantum circuits,” (2022), arXiv:2209.06069 [quant-ph].
- [36] XanaduAI, “Mrmustard,” <https://github.com/XanaduAI/MrMustard> (2023).
- [37] Nathan Killoran, Josh Izaac, Nicol as Quesada, Ville Bergholm, Matthew Amy, and Christian Weedbrook, “Strawberry Fields: A Software Platform for Photonic Quantum Computing,” *Quantum* **3**, 129 (2019).
- [38] X. Valcarce, P. Sekatski, E. Gouzien, A. Melnikov, and N. Sangouard, “Automated design of quantum-optical experiments for device-independent quantum key distribution,” *Phys. Rev. A* **107**, 062607 (2023).
- [39] Mario Krenn, Manuel Erhard, and Anton Zeilinger, “Computer-inspired quantum experiments,” *Nature Reviews Physics* **2**, 649–661 (2020).
- [40] Carlos Ruiz-Gonzalez, S oren Arlt, Jan Petermann, Sharareh Sayyad, Tareq Jaouni, Ebrahim Karimi, Nora Tischler, Xuemei Gu, and Mario Krenn, “Digital discovery of 100 diverse quantum experiments with pytheus,” *Quantum* **7**, 1204 (2023).
- [41] Alexey A. Melnikov, Pavel Sekatski, and Nicolas Sangouard, “Setting up experimental bell tests with reinforcement learning,” *Physical Review Letters* **125** (2020), 10.1103/physrevlett.125.160401.

Appendix A: 2-outcomes POVM for qubits implemented with homodyne measurement

a. Qubit POVM A Positive operator-valued measured (POVM) with k outcomes is a set of Hermitian operator $\{E_i\}_{i=1}^k$ which are positive $E_i \geq 0 \forall i$ and satisfy the normalisation condition $\sum_i E_i = I$. In the case of qubits one can write an arbitrary Hermitian operator in the Bloch form:

$$E_i = \lambda_i (\mathbb{1} + \vec{n}_i \cdot \vec{\sigma}) \quad (\text{A1})$$

where $|\vec{n}_i| \leq 1$. In the case of 2-outcomes the normalisation condition impose that $\sum_i \lambda_i \vec{n}_i = 0$ thus $\vec{n}_1 = -\frac{|\vec{n}_2|}{|\vec{n}_1|} \vec{n}_2$ and $\lambda_1 + \lambda_2 = 1$. One can rewrite such POVM as a convex mixture of extremal POVM:

$$\begin{aligned} E_1 &= \mu |\vec{n}\rangle \langle \vec{n}| + (1 - \mu) r_1 \mathbb{1}, \\ E_2 &= \mu |-\vec{n}\rangle \langle -\vec{n}| + (1 - \mu) r_2 \mathbb{1} \end{aligned} \quad (\text{A2})$$

where $|\vec{n}\rangle \langle \vec{n}| = \vec{n} \cdot \vec{\sigma}$, $\mu = 2|n_i| \lambda_i$ and $r_i = \frac{(\lambda_i - \mu)}{1 - \mu}$. μ represent the projective part of the POVM, $(1 - \mu)$ the random part and $|\pm \vec{n}\rangle$ is the eigenvector associated to the ± 1 eigenvalue of $\vec{n}_i \cdot \vec{\sigma}$.

b. Optimizing the trace distance The trace distance μ_h defined in section III reads:

$$\mu_h = \frac{1}{2} \int ||p(\theta, |\vec{n}\rangle) - p(\theta, |-\vec{n}\rangle)||. \quad (\text{A3})$$

The maximum of μ_H is achieved when $D(x, m, l, \phi, a, \theta) = ||p(\theta, |\vec{n}\rangle) - p(\theta, |-\vec{n}\rangle)||$ is maximum, the explicit expression of $D(x, m, l, \phi, a, \theta)$ being

$$\begin{aligned} D(x, m, l, \phi, a, \theta) &= \\ & \left| \left| e^{-x^2} \left(\frac{2 \sin(2a) H_l(x) H_m(x) \cos(\theta m - \theta l + \phi)}{\sqrt{\pi} \sqrt{2^m m!} \sqrt{2^l l!}} \right) \right. \right. \\ & \left. \left. + \cos(2a) \left(\frac{2^{-n} H_l(x)^2}{\sqrt{\pi} l!} - \frac{2^{-m} H_m(x)^2}{\sqrt{\pi} m!} \right) \right| \right| \end{aligned} \quad (\text{A4})$$

Where the states $|\pm n\rangle$ are parametrized as

$$|\vec{n}\rangle = \cos(a) |l\rangle + e^{i\phi} \sin(a) |m\rangle \quad (\text{A5})$$

$$|-\vec{n}\rangle = \cos(a) |l\rangle - \sin(a) e^{i\phi} |m\rangle. \quad (\text{A6})$$

The maximum value of $D(x, m, l, \phi, a, \theta)$ over ϕ , a and θ is necessarily achieved when $|\cos(\theta m - \theta l + \phi)| = 1$, so $\theta m - \theta l + \phi = 0$ or π . The first case corresponds to $\theta = 0$ and $\phi = 0$ and the second case π can be brought back to the first one by changing a into $-a$ in Eq. (A4). Therefore, we have that:

$$\max_{\phi, a, \theta} \mu_H = \max_{\phi=0, a, \theta=0} \mu_H. \quad (\text{A7})$$

The worst case scenario, in order to violate the CHSH inequality with measurement of the form Eq. (A2) is to have $r_1 + r_2 = \frac{1}{2}$ in this case we use the correlator

$$\sigma_{|\vec{n}\rangle} = \mu (|\vec{n}\rangle \langle \vec{n}| - |-\vec{n}\rangle \langle -\vec{n}|). \quad (\text{A8})$$

We consider the case where Alice and Bob are using the same settings, the corresponding CHSH operator

$$\begin{aligned} \mathbb{B} &= \sigma_{|\vec{n}_1\rangle} \sigma_{|\vec{n}_1\rangle} \\ &+ \sigma_{|\vec{n}_1\rangle} \sigma_{|\vec{n}_2\rangle} \\ &+ \sigma_{|\vec{n}_2\rangle} \sigma_{|\vec{n}_1\rangle} \\ &- \sigma_{|\vec{n}_2\rangle} \sigma_{|\vec{n}_2\rangle} \end{aligned} \quad (\text{A9})$$

The maximum value of the CHSH inequality is achieved when measure with the operator Eq. (A9) is obtain where the Bloch vector of $|\vec{n}_1\rangle$ and $|\vec{n}_2\rangle$ are orthogonal. We showed that the maximum of μ_h is achieved for a real state $|\vec{n}\rangle$. Let a_{max} be the optimal value of a for the optimization Eq. (A7). The corresponding state is

$$|\vec{n}_1\rangle = \cos\left(\frac{a_{max}}{2}\right) |l\rangle + \sin\left(\frac{a_{max}}{2}\right) |m\rangle. \quad (\text{A10})$$

We write $|\vec{n}_2\rangle$ as

$$|\vec{n}_2\rangle = \cos\left(\frac{a_2}{2}\right) |l\rangle + e^{i\phi_2} \sin\left(\frac{a_2}{2}\right) |m\rangle. \quad (\text{A11})$$

One can see from Eq. (A4) that one can always chose θ such that $D(x, m, l, \phi, a, \theta) = D(x, m, l, 0, a, 0)$ we then choose $a_2 = a_{max}$ and get $\mu_{\vec{n}_2} = \mu_{\vec{n}_1}$ for all ϕ_2 . Finally the condition on a_{max} for which it exist a ϕ_2 such that the Bloch vector of $|\vec{n}_2\rangle$ and $|\vec{n}_1\rangle$ are orthogonal is $|\cos(a_{max})|^2 \leq \frac{1}{2}$. Therefore for all $\mu_{|\vec{n}\rangle}$ such that $|\cos(a)|^2 \leq \frac{1}{2}$ One can achieve the CHSH violation of

$$S = \mu^2 2\sqrt{2}. \quad (\text{A12})$$

c. Certification of best possible quantum bound In order to obtain the best possible score to a Bell inequality, the states retained should be as distinguishable as possible, which means that their overlap should be as small as possible. With previous notations, considering two orthogonal states, μ can be optimized so that it exactly quantifies the overlap between them. Besides, there is a threshold value μ_t that certifies that the local bound can be exceeded. But for a fixed value of μ , the values r_i can be optimized also. Loosely speaking, they represent the best way to construct a POVM, taking into account the difference between the values of the two probability densities within the area where they overlap. In order to formalize these ideas, let us consider the two following probability densities:

$$f(x) = |\langle x | \vec{n} \rangle|^2, \quad g(x) = |\langle x | -\vec{n} \rangle|^2 \quad (\text{A13})$$

where $|\vec{n}\rangle$ and $|-\vec{n}\rangle$ have been defined just above. Let us consider the POVM associated to an homodyne detection. We can write once again in two different ways, in the $\{|\vec{n}\rangle, |-\vec{n}\rangle\}$ basis.

$$\begin{aligned} E_1 &= \begin{bmatrix} \int_A f(x) & 0 \\ 0 & \int_A g(x) \end{bmatrix} \\ &= \begin{bmatrix} \mu + (1 - \mu)r_1 & 0 \\ 0 & (1 - \mu)r_1 \end{bmatrix} \end{aligned} \quad (\text{A14})$$

where A is the interval chosen for the binning. It yields

$$\mu = \int_A f - g, \quad r_1 = \frac{\int_A g}{1 - \int_A (f - g)} \quad (\text{A15})$$

Finally, in order to prove that the best numerical result is always obtained by an optimization on the projective part only, we have to show that the value of the random part r_1 is controlled, that is upper bounded, whenever the projective part μ is above a certain value. The final problem is written:

$$\begin{aligned} \max_A & \frac{\int_A g}{1 - \int_A (f - g)} \\ \text{s.t.} & \int_A (f - g) > \mu_c \\ & f, g \in \mathcal{H}_2 \end{aligned}$$

where $\mathcal{H}_2 = \{|\lambda_{n_1} H_{n_1}(x) + \lambda_{n_2} H_{n_2}(x)|^2 | \lambda_{n_1} + \lambda_{n_2} = 1\}$.

Appendix B: Noise Model for operators

In this section, we propose to test the robustness of the violations with regard to experimental conditions. The most common source of noise in these experiments are photon losses, which can be modelled by the action of a beam-splitter which entangles an ideal incoming state with an ancillary fluctuating quantum field, in that case the void state $|0\rangle$. After recombination on the beam-splitter, two outputs are produced corresponding to the transmitted part of the beam-splitter and to the reflected one. In order to obtain the noisy operator, we trace-out the part corresponding to the reflection. Hence, stemming from the ideal observable:

$$\hat{O} = +1 \int_E dX |X\rangle \langle X| - 1 \int_{\bar{E}} dX |X\rangle \langle X| \quad (\text{B1})$$

our final goal is to compute:

$$\langle 0 | \hat{U} \hat{O} \hat{U}^\dagger | 0 \rangle \quad (\text{B2})$$

where \hat{U} is the beam-splitter observable defined by $\hat{U} = e^{i\theta(\hat{a}^\dagger \hat{b} - \hat{a} \hat{b}^\dagger)}$, \hat{a}, \hat{b} are the annihilation operators respectively on the first and second mode, and the reflection is $\eta = \cos(\theta)^2$. We use

$$|X\rangle \langle X| = \frac{1}{2\pi} \int_{\mathbb{R}} e^{i\xi(\hat{x}-x)} \quad (\text{B3})$$

and

$$\hat{x} = \frac{\hat{a} + \hat{a}^\dagger}{\sqrt{2}} \quad (\text{B4})$$

and with $\hat{A} = i\theta(\hat{a}^\dagger \hat{b} - \hat{a} \hat{b}^\dagger)$ and $\hat{B} = \frac{i\xi(\hat{a} + \hat{a}^\dagger)}{\sqrt{2}}$ the quantity to compute is now:

$$\int_I dX |X\rangle \langle X| = \int_I \frac{dx}{2\pi} \int d\xi e^{-i\xi x} d\xi e^{\hat{A}} e^{\hat{B}} e^{-\hat{A}}. \quad (\text{B5})$$

We are going to first develop the product of the exponential of operators under the integral. To begin with, let us note that, with $K_\xi = \frac{i\xi}{\sqrt{2}}$

$$[K_\xi \hat{a}, K_\xi \hat{a}^\dagger] = \frac{\xi^2}{2} \mathbf{1} \quad (\text{B6})$$

and since this commutator commutes with $K_\xi \hat{a}$ and $K_\xi \hat{a}^\dagger$, the Baker-Campbell-Hausdorff formula yields :

$$\exp(\hat{B}) = \exp(K_\xi \hat{a}) \exp(K_\xi \hat{a}^\dagger) \exp\left(\frac{-\xi^2}{4}\right). \quad (\text{B7})$$

We use

$$e^{\hat{A}} e^{-\hat{A}} = \mathbf{1} \quad (\text{B8})$$

to finally rewrite $e^{\hat{A}} e^{\hat{B}} e^{-\hat{A}}$ as:

$$\begin{aligned} \exp\left(\frac{-\xi^2}{4}\right) \exp(\hat{A}) \exp(K_\xi \hat{a}) \exp(-\hat{A}) \\ \times \exp(\hat{A}) \exp(K_\xi \hat{a}^\dagger) \exp(-\hat{A}) \end{aligned} \quad (\text{B9})$$

The Campbell identity yields:

$$\exp(\hat{A}) \exp(K_\xi \hat{a}) \exp(-\hat{A}) = \sum_{n=0}^{\infty} \frac{[(\hat{A})^n, K_\xi \hat{a}]}{n!} \quad (\text{B10})$$

where $[(\hat{A})^n, K_\xi \hat{a}] = [\hat{A}, \dots, [\hat{A}, [\hat{A}, K_\xi \hat{a}]]]$. We separate this sum into its even and its odd parts, and use the fact that:

$$[(\hat{A})^{2p}, K_\xi \hat{a}] = K_\xi (i\theta)^{2p} \hat{a} \quad (\text{B11})$$

and

$$[(\hat{A})^{2p+1}, K_\xi \hat{a}] = K_\xi (i\theta)^{2p+1} \hat{b} \quad (\text{B12})$$

to finally obtain:

$$\begin{aligned} \exp(\hat{A}) \exp(K_\xi \hat{a}) \exp(-\hat{A}) \\ = \sum_{p \geq 0} \frac{(i\theta)^{2p}}{(2p)!} \hat{a} + \sum_{p \geq 0} \frac{(i\theta)^{2p+1}}{(2p+1)!} \hat{b} \\ = K_\xi \left(\cosh(i\theta) \hat{a} + \sinh(i\theta) \hat{b} \right) \\ = K_\xi \left(\cos(\theta) \hat{a} + \sin(\theta) \hat{b} \right). \end{aligned} \quad (\text{B13})$$

Now, using Eq. Eq. (B13) and Eq. Eq. (B9), we have that Eq. Eq. (B5) is equal to:

$$\begin{aligned} \int_I \frac{dx}{2\pi} \int d\xi \left(e^{-i\xi x} \right. \\ \times e^{\frac{-\xi^2}{4}} e^{K_\xi (\cos(\theta) \hat{a}^\dagger + \sin(\theta) \hat{b}^\dagger)} \\ \left. \times e^{K_\xi (\cos(\theta) \hat{a} + \sin(\theta) \hat{b})} \right) \end{aligned} \quad (\text{B14})$$

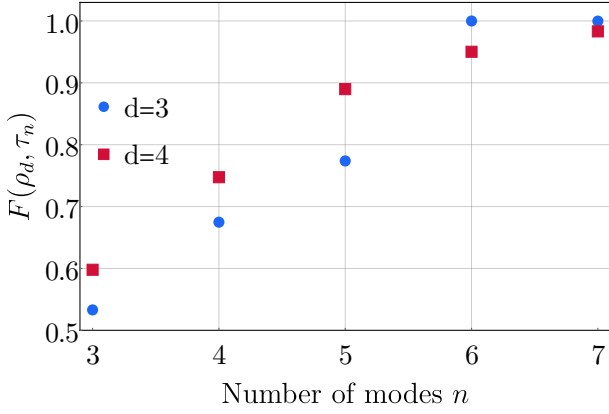


FIG. 6. Optimized fidelities $F(\rho_d, \tau_n)$ given for local dimensions $d = 3$ and $d = 4$ and for circuits of $n = \{3, 4, 5, 6, 7\}$ modes circuits.

Finally, we apply $\langle 0| \cdot |0\rangle$ and Eq. Eq. (??) becomes:

$$\int_E \frac{dx}{2\pi} \int d\xi e^{-i\xi x} e^{\frac{-\xi^2}{4}} \exp^{K_\xi \cos(\theta) \hat{a}^\dagger} \exp^{K_\xi \cos(\theta) \hat{a}} \quad (\text{B15})$$

For any $(k, n) \in \mathbb{N}^2, k \leq n$,

$$\hat{a}^k |n\rangle = \sqrt{(n)}\sqrt{(n-1)}\dots\sqrt{(n-k-1)} |n-k\rangle \quad (\text{B16})$$

So

$$\begin{aligned} & \exp(K_\xi \cos(\theta) \hat{a}) |n\rangle \\ &= \sum_{k=0}^{\infty} \frac{(K_\xi \cos(\theta) \hat{a})^k}{k!} |n\rangle \\ &= \sum_{k=0}^n \frac{(K_\xi \cos(\theta))^k \sqrt{\binom{n}{k}} |n-k\rangle}{\sqrt{k!}} \end{aligned} \quad (\text{B17})$$

Appendix C: Realistic implementation of Bell violation with homodyne measurements

To study the feasibility of implementing states yielding a high CHSH score, we consider circuits using one Gaussian operation \mathcal{G} with zero-displacement followed by displacement operations, as shown in Fig. 4. For local dimension $d = 3, 4$ and for circuits up to $n = 7$ modes, we give the optimized fidelity $F(\rho_d, \tau_n)$ over circuits parameters in Fig. 6. For these circuits, we also provide in Fig. 7 the heralding probability, i.e. the probability to obtain a detection event on all $n - 2$ last modes simultaneously. In order to better understand the experimental resources needed for the proposed implementations, we here provide optimal circuit parameters in terms of squeezing and displacement amplitudes.

For clarity, we first define squeezing and displacement operations. Single-mode squeezing operations on mode i

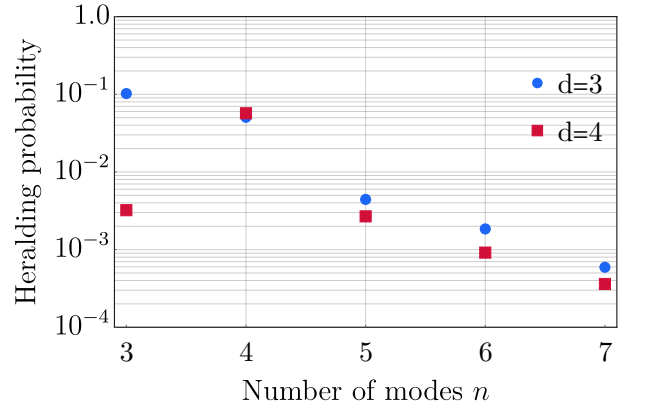


FIG. 7. Heralding probability for circuits achieving the best fidelities for local dimensions $d = 3$ and $d = 4$ and using $n = \{3, 4, 5, 6, 7\}$ modes.

act following

$$S(z) = \exp\left(\frac{1}{2}(z^* \hat{a}_i^2 - z(\hat{a}_i^\dagger)^2)\right), \quad (\text{C1})$$

where \hat{a}_i and \hat{a}_i^\dagger are the ladder operators of mode i , and $z = r \exp(i\phi)$ with $r \in \mathbb{R}$ and $\phi \in [0, 2\pi]$. Displacement operations on mode i are given by

$$D(\alpha) = \exp\left(\alpha \hat{a}_i - \alpha^* \hat{a}_i^\dagger\right), \quad (\text{C2})$$

with $\alpha \in \mathbb{C}$.

To obtain the squeezing parameter from the unitary \mathcal{G} we use the Bloch-Messiah decomposition [30, 31]. In phase-space, the transformation \mathcal{G} is fully characterized by a symplectic matrix $\Omega \in \mathbb{R}^{2n \times 2n}$. The Bloch-Messiah decomposition implies that Ω can be written as $\Omega = O_1 Z O_2$, with O_1, O_2 two orthogonal symplectic matrices, and Z a diagonal matrix. Moreover, when acting on the vacuum, as it is the case in setups we consider, the orthogonal property of O_1 and O_2 allow us to simplify the expression to

$$\mathcal{G} = O_1 Z. \quad (\text{C3})$$

O_1 can be interpreted as passive Gaussian transformations, i.e. as a combination of phase-shifters and beam-splitters, while $Z = \text{diag}(\exp(-r_1), \dots, \exp(-r_n), \exp(r_1), \dots, \exp(r_n))$ represents an array of single-mode squeezer acting with parameter $z = r_i$ on mode i .

We use the Bloch-Messiah decomposition implemented in STRAWBERRYFIELDS [37]. In Table I, we give the optimal squeezing and displacement parameters when optimizing ρ_3 for circuits up to $n = 7$ -modes. These parameters are given for circuits targeting ρ_4 in Table II.

While no constraints are set on the squeezing parameters, we found a maximum squeezing of $r \approx 2.3$. Using

$$V_{\text{dB}} = -10 \times \log_{10}(\exp(-2r)), \quad (\text{C4})$$

mode	1	2	3	4	5	6	7
	Squeezing parameter r						
n=3	0.6872	0.6631	0.3934				
n=4	1.2387	1.1164	0.6693	0.5484			
n=5	2.2971	1.3560	1.1815	0.4920	0.2930		
n=6	1.4834	1.2309	0.7445	0.6903	0.5410	0.2405	
n=7	1.1953	1.1670	0.7855	0.6586	0.6285	0.3194	0.2701
	Displacement d						
n=3			0.5089				
n=4			0.3527	-0.3077			
n=5			0.7174	-0.4598	0.4729		
n=6			0.4847	-0.4373	0.4958	-0.4986	
n=7			0.4781	-0.5003	0.4906	-0.4955	0.4785

TABLE I. Circuits parameters maximizing the fidelity $F(\rho_3, \tau_n)$ when considering $n = 3, 4, 5, 6, 7$ bosonic modes.

mode	1	2	3	4	5	6	7
	Squeezing parameter r						
n=3	2.0618	0.6903	0.1571				
n=4	1.1707	1.1027	0.8939	0.3295			
n=5	1.6180	1.3506	0.9420	0.6105	0.3116		
n=6	1.7885	1.0188	0.9710	0.8686	0.5690		
n=7	1.4353	1.0714	0.8333	0.6945	0.6392	0.2438	
	Displacement d						
n=3			0.3862				
n=4			0.4927	-0.5405			
n=5			0.4326	-0.4696	0.4467		
n=6			0.4959	-0.5035	0.5029	-0.5790	
n=7			0.4137	-0.4120	0.4019	-0.5450	0.4990

TABLE II. Circuits parameters maximizing the fidelity $F(\rho_4, \tau_n)$ when considering $n = 3, 4, 5, 6, 7$ bosonic modes.

this corresponds to 20dB squeezed vacuum states. Importantly, the $n = 6$ -modes circuit preparing exactly the state $\rho_{d=3}$ only requires $r \leq 1.485$ or 12.9dB of squeezing. In the $d = 4$ case, the 7-mode photonic circuits needs $r \leq 1.435$ or 12.5dB squeezed vacuum states. This is well below experimental limits, as direct observations of up 15dB squeezing have been reported [28]. Note that more refined approaches to design photonic circuits, e.g. see [38–41], might be necessary to better match or ease other experimental constraints for the preparation of the proposed quantum states. More specifically, such method could be used in combination with the optimisation Eq. (18) to directly target a high CHSH score.